HHS Public Access

Author manuscript

J Invest Dermatol. Author manuscript; available in PMC 2021 June 01.

Published in final edited form as:

J Invest Dermatol. 2020 June ; 140(6): 1204–1213.e5. doi:10.1016/j.jid.2019.10.013.

Overexpression of MYB in the skin induces alopecia and epidermal hyperplasia

Yuan Hu[1,2,3], **Zhongya Song**[4,5], **Jiang Chen**[4], **Carlos Caulin**[1,2,6,*]

[1]Department of Otolaryngology - Head & Neck Surgery, The University of Arizona, Tucson, AZ 85724, USA.

[2]Department of Head and Neck Surgery, The University of Texas MD Anderson Cancer Center, Houston, TX 77030, USA.

[3]Department of Otolaryngology, Union Hospital, Tongji Medical College, Huazhong University of Science and Technology, Wuhan, Hubei 430022, China.

[4]Department of Pathology Stony Brook Medicine, Stony Brook University School of Medicine, NY 11794, USA.

[5]Department of Dermatology, Peking University First Hospital, Beijing, China, 100034.

[6]The University of Arizona Cancer Center, Tucson, AZ 85724, USA

Abstract

The skin homeostasis is controlled by a complex interplay between tightly regulated transcription factors and signaling pathways. MYB is a transcription factor expressed in hair follicle progenitor cells and found overexpressed in adnexal skin tumors. However, the biological consequences of deregulated MYB expression in the skin remain poorly understood. To address this, we generated transgenic mice that overexpress MYB in epidermal and follicular keratinocytes. These mice exhibited a normal hair coat after birth, but gradually developed alopecia, accompanied by altered follicular differentiation, disrupted hair cycle and a marked depletion of hair follicle stem cells. Additionally, transgenic mice developed massive epidermal hyperplasia and hyperkeratosis. Global expression profiling not only confirmed that the skin of these mice exhibited transcriptomic

[*]**Corresponding author:** Carlos Caulin, PhD, Department of Otolaryngology - Head & Neck Surgery. The University of Arizona Cancer Center, 1515 N. Campbell Avenue, Tucson, AZ 85724, USA. Phone: (520)-626-6078; Fax: (520) 626-6995; ccaulin@oto.arizona.edu.

CRediT STATEMENT (AUTHOR CONTRIBUTIONS)

Conceptualization: CC, JC**; Data curation:** YH, ZS, CC, JC; **Formal analysis:** YH, CC; **Funding acquisition:** CC, JC**; Investigation:** YH, ZS**; Methodology:** YH, ZS, CC, JC; **Project administration:** CC**; Resources:** CC, JC**; Software:** CC**; Supervision:** CC, JC**; Validation:** YH, ZS, CC, JC; **Visualization:** YH, ZS, CC, JC; **Writing – original draft:** CC; **Writing – review & editing:** YH, ZS, JC

DATA AVAILABILITY STATEMENT

RNaseq data was deposited in the Sequence Read Archive (SRA) under accession number PRJNA574690. Any additional data is available from the corresponding author upon reasonable request.

CONFLICT OF INTEREST

The authors declare no conflict of interest.

features of alopecia and epidermal differentiation, but also revealed features of psoriasis and the inflammatory response. The latter was further confirmed by the increased T cell infiltration found in the skin of transgenic mice. Overall, these results suggest that tight regulation of MYB expression in the skin is critical to maintain skin homeostasis.

INTRODUCTION

The skin architecture and function is maintained by a delicate balance between proliferation and differentiation (Blanpain and Fuchs, 2009). Imbalances in these processes may result in structural and functional alterations in the epidermis and its appendages, leading to skin disorders (Lopez-Pajares et al., 2013, Mills et al., 2018).

Over the past years, the molecular pathways that control epidermal and hair follicle homeostasis have been extensively dissected (Eckhart et al., 2013, Kobielak et al., 2007, Lim and Nusse, 2013, Zhang et al., 2006). Those studies and multiple transcriptomic analyses identified genes preferentially expressed in specific cell populations of the epidermis and hair follicles, many of which encode for transcription factors that regulate complex gene expression programs in the skin (Cheng et al., 2018, Joost et al., 2016, Yang et al., 2017). The mRNA expression of the *Myb* gene, encoding for the MYB transcription factor, was also identified in those studies as being enriched in hair progenitors cells in embryonic skin (Rhee et al., 2006), and in the stem cell niche (bulge) of the hair follicle in adult mice (Adam et al., 2018). Previous studies had also found *Myb* mRNA expression in the matrix cells of anagen hair follicles (Ess et al., 1999). The MYB protein was detected at postnatal day 5 (P5) immediately under the bulge in the outer root sheath (ORS), an area occupied by transit amplifying cells, and in the hair matrix, but it was undetected at later time points (Vesela et al., 2014). Overall, the data suggest that tight regulation of MYB expression may be required to maintain the hair follicle homeostasis.

MYB overexpression has also been observed in cutaneous adnexal neoplasms, a group of benign and malignant tumors that exhibit morphological differentiation towards one or more types of the skin adnexal structures, such as the hair follicles, sebaceous and sweat glands, suggesting that MYB overexpression may disrupt the skin homeostasis and eventually contribute to tumor development (Alsaad et al., 2007, Evangelista and North, 2017, Rajan et al., 2016, van der Horst et al., 2015). However, the consequences of deregulated MYB expression in the skin have not been studied.

In this study, we generated transgenic mice that overexpress MYB in epidermal and follicular keratinocytes, to assess the biological consequences of deregulated MYB expression in the skin and to identify genes and pathways that may mediate pathological responses to constitutive MYB expression. We found that MYB overexpression induces epidermal hyperplasia, alopecia, impaired hair follicle cycle and differentiation, depletion of hair follicle stem cells, and psoriasis-like inflammatory responses.

RESULTS

MYB overexpression in skin keratinocytes promotes hair loss

To determine the biological consequences of deregulated MYB expression in the skin, we generated mice that overexpress MYB in skin keratinocytes, using the TetO system. These mice were generated by crossing TetO-Myb mice with R26.ZtTA and K5.CrePR1 mice (Li et al., 2010, Zhou et al., 2002) to generate trigenic TetO-Myb; R26.ZtTA; K5CrePR1 mice (K5-Myb mice hereafter) (Fig. S1a–b). Control mice in this study included bigenic and monogenic littermates, as indicated (Table S1).

Elevated MYB protein expression in the skin of K5-Myb mice was confirmed by western blotting, using two different antibodies (Fig. 1a). In situ hybridization demonstrated that in control mice endogenous *Myb* mRNA was expressed predominantly in hair matrix keratinocytes of anagen hair follicles (P15 and P35) (Figs. 1b and S2a). *Myb* was also expressed at low levels in the ORS of the hair follicle and in basal epidermal keratinocytes at P15 (Fig. S2a), but it was undetectable in these areas in anagen hair follicles at P35 (Fig. 1b). Endogenous *Myb* mRNA was below detection in telogen hair follicles and adult epidermis of control mice (P45), suggesting that the *Myb* expression in the skin is dynamically regulated. In transgenic mice, *Myb* was robustly expressed throughout the proximal hair follicles, the distal ORS and infundibulum, and patches of basal and spinous/granular layers of the epidermis (Figs. 1b and S2a). The expression pattern of MYB protein, as demonstrated by immunohistochemistry, was similar to that of the *Myb* mRNA, (Figs. 1b and S2a).

The K5-Myb mice developed a normal first hair coat (Figs. 1c and S2b, P15 and P24), but we noticed that adult mice started to lose their hair by P45 (Figs. 1c and S2b). At P90, K5-Myb mice had undergone massive hair loss and only small patches of hair remained, and by P210 only sporadic hairs were observable (Fig. 1c). These mice were monitored for up to 18 months and their hair never grew back, indicating that MYB overexpression induced a permanent hair loss (Fig. S2b). Control mice (Table S1) had a normal hair coat for the duration of the investigation (Figs. 1c and S2b).

MYB overexpression disrupts hair follicle differentiation and hair cycle, and induces epidermal hyperplasia

Histologically, the epidermis and postnatal hair follicle morphogenesis (P15) was similar in K5-Myb and control mice (Fig. S3a). By P35, the regenerated hair follicles in the first anagen appeared atrophic in K5-Myb mice (Fig. 2a). Hair follicles were abnormally curved and hair medulla was disorganized, suggesting impaired hair follicle differentiation. These changes were progressive and by P90 few or no typical anagen hair follicles were visible (Fig. 2a). First and second telogen, as examined at P24 and P45, occurred normally in K5-Myb mice, but the second anagen began early in these mice. Overall, these findings indicate that MYB overexpression in skin keratinocytes disrupts the hair cycle (Figs. 2a and S3b).

By P24, the epidermis of K5-Myb mice became hyperplastic and hyperkeratotic (Fig. 2a). The spinous layer was expanded and the stratum corneum thickened. BrdU incorporation confirmed the increased proliferation in the epidermis of K5-Myb mice by P24, primarily

confined to the basal layers of the epidermis (Figs. 2b–c and S3c). On the other hand, BrdU incorporation in hair matrix cells under the line of Auber was comparable in K5-Myb and control mice (Figs. 2b and S3d).

Immunofluorescence analysis of epidermal differentiation revealed that the basal layers, labeled with keratin 14 (KRT14), suprabasal layers labeled with Keratin 10 (KRT10) and granular layers labeled with involucrin (INV), were consistently expanded from P24 (Figs. 3 and S4). The expression pattern of loricrin (LOR), on the other hand, did not change until P90, when expansion of the LOR layers was also observed. These observations suggest an increased proliferation and differentiation in the epidermis of K5-Myb mice.

Hair follicle differentiation markers were analyzed by immunofluorescence (Fig. 4a). The ORS (KRT14) and companion layer (KRT75) of K5-Myb were relatively normal at both P35 and P90, except that the companion layer was more curvy in P90 K5-Myb mice. Hair cortex was severely disrupted (curvy and irregular) as demonstrated by low and discontinuous AE15, AE13, and KRT71 staining. For those hair follicles that contained hair medulla, the medulla was discontinuous and exhibited irregular expression of trichohyalin (labeled by AE15). The hair shaft cuticle (KRT82) was formed but was also curvy. Overall, the differentiation of inner root sheath and hair shaft was impaired in K5-Myb mice, resulting in abnormal structures.

Hair follicle stem cell depletion in the skin of mice that overexpress MYB

Abnormal hair follicle differentiation and progressive hair loss prompted us to examine hair follicle stem cells with an antibody for KTR15, a marker of hair follicle bulge stem cells (Liu et al., 2003). At P45, when most hair follicles were in telogen, KTR15-positive cells were significantly reduced in K5-Myb hair follicles (Fig. 4b). Similarly, the hair follicle stem cell markers CD34 (Trempus et al., 2003) and NFATc1 (Horsley et al., 2008, Tumbar et al., 2004) were also found downregulated in hair follicles of K5-Myb mice (Fig. 4c). These findings indicate that MYB overexpression in skin keratinocytes could result in the depletion of hair follicle stem cells.

Gene expression profiles induced by MYB overexpression

To gain additional insight into the molecular and phenotypic changes induced by MYB overexpression in the skin, we generated RNAseq expression profiles from the skin of K5-Myb and control mice at 12 months of age, when the K5-Myb skin phenotypes had been established and proven to be irreversible. Unsupervised cluster analysis showed distinct transcriptomes for the K5-Myb and control samples (Fig. S5a). Differential expression analysis identified 1,057 upregulated genes and 1313 downregulated genes in the skin of K5-Myb mice, with an adjusted p-value <0.01 (Table S2). As expected, Myb was one of the top overexpressed genes, accompanied by upregulation of genes involved in late epidermal terminal differentiation, such as filaggrin (Flg), loricrin (Lor), late cornified envelope genes (Lce1 and Lce3) or hornerin (Hrnr) (Fig. 5a and Table S2).

Interestingly, multiple genes, including transcription factors, that control hair follicle differentiation (e.g. Msx2, Bmp2, Bmp4, Foxn1, Efl5, Hoxc13 and Lhx2) were found downregulated in the skin of K5-Myb mice (Figs. 5a and Table S2). Quantitative RT-PCR

validated these findings (Figs. 5b and S5b). Of those genes, only Msx2, Bmp2, Bmp4 were also found downregulated at P15, when MYB was overexpressed (Figs. S2a and S4b), but before the onset of the phenotypic changes (Figs. 5b and S5b), suggesting that early changes in these transcriptional regulators are more likely to be a primary consequence of MYB overexpression, while late changes may be secondary events.

To better understand the significance of these changes in gene expression, we analyzed functional enrichment using the ToppGene Suite (Chen et al., 2009). This analysis revealed that genes involved in hair cycle were highly downregulated in the skin of K5-Myb, along with keratin filament genes, many of which were hair keratins and keratin-associated protein genes (Krtap) (Figs. 5c and Table S3), which may underlie the hair differentiation defects observed in these mice. Analysis of human disease and phenotypes revealed that “hypotrichosis” and “alopecia” were two of the leading terms enriched for these categories, consistent with the hair loss observed in K5-Myb mice. Of note, analysis of the Coexpression Atlas identified several gene sets for genes overexpressed in embryoid bodies compared to stem cells and fibroblasts that were enriched in genes downregulated in the K5-Myb skin, suggesting the possibility MYB overexpression might impact the stem cell function.

“Keratinization” and “keratinocyte differentiation” were the top gene ontology (GO) terms enriched in upregulated genes, associated with molecular pathways involved in the formation of the cornified envelope (Fig. 5d and Table S4). In addition, we found that the “immune” and “inflammatory response” were highly enriched GO terms for upregulated genes, accompanied by “cytokine-cytokine receptor interactions” and “signaling by interleukins” pathways. Interestingly, “psoriasis” and “eczema” were the top two diseases enriched for upregulated genes, with highly significant q-values, suggesting that MYB overexpression may upregulate the expression of genes involved in these inflammatory skin disorders.

Gene Set Enrichment Analysis (GSEA) revealed that the IL23 pathway was the most significantly enriched for upregulated genes, and the BMP pathway was the most significant for downregulated genes in the skin of K5-Myb mice (Fig. 5e). Given the detrimental role of IL23 in skin inflammatory disorders (Cargill et al., 2007, Lee et al., 2004, Nair et al., 2009, Nair et al., 2008), and the regulatory function of BMP signaling in hair differentiation (Botchkarev et al., 2001, Guha et al., 2004, Kulessa et al., 2000, Rendl et al., 2008), it is speculated that impairment in these pathways in K5-Myb mice might have contributed to the skin phenotypes.

Immune infiltration in the skin of K5-Myb mice

To confirm the immune-related GO terms found in the RNAseq analysis we stained the skin of K5-Myb and control mice with an antibody for CD3 as a marker for T-cells (Fig. 6a–b). We found that T-cell infiltration was much more prominent in the skin of K5-Myb mice than in control mice, confirming that overexpression of MYB in the epidermis promotes immune cell infiltration. Interestingly, significant T-cell infiltration was found at P15, before gross and histological phenotypes were observed (Fig. 6b). In addition, we observed that FOXP3, a marker for immunosuppressive regulatory T-cells (Tregs) was also significantly higher in

the K5-Myb skin, suggesting that immune cell infiltration, which may promote immunity, is accompanied by recruitment of immune suppressive T-cells that may counteract these immune protective effects.

DISCUSSION

To understand the biological consequences of deregulated MYB expression in the skin, we generated transgenic mice that overexpress MYB in epidermal and follicular keratinocytes. We found that these mice developed epidermal hyperplasia and hyperkeratosis, hair loss, disrupted hair follicle cycle and differentiation, hair follicle stem cell depletion and cutaneous immune cell infiltration. Molecular characterization supported these phenotypes and suggested that the skin of MYB-overexpressing mice resembles at the molecular and pathological levels the features of those found in inflammatory skin disorders such as psoriasis and eczema. The data indicates that timely regulation of MYB expression in cutaneous keratinocytes is required to maintain skin homeostasis.

The K5-Myb mice underwent hair loss after they had developed a normal first hair coat. This phenotype was accompanied by abnormal hair follicle differentiation and hair follicle stem cell depletion. These phenotypes were consistent with the skin gene expression profiles of K5-Myb mice, included the strong downregulation of hair follicle keratins such as Krt84 and Krt74 (Table S2), multiple hair-specific keratin-associated proteins, structural proteins that integrate the mature hair follicle encoded by Krtap genes (Liu et al., 2016), and a number of transcription factors involved in hair follicle differentiation such as Hoxc13, Lhx2, Foxn1, or Msx2 (Godwin and Capecchi, 1998, Jiang et al., 1999, Millar, 2002, Rhee et al., 2006, Tkatchenko et al., 2001) (Table S2).

In addition, downregulation of the BMP pathway was noted in the skin of K5-Myb mice. Interestingly, we observed that Bmp2, Bmp4 and Msx2 were downregulated at P15 in K5-Myb mice, before the hair phenotypes developed, whereas the expression of Hoxc13, Lhx2, Foxn1 and Elf5, did not change until after the phenotypes were detected. While future studies will be required to precisely identify the genes that are directly regulated by MYB that may initiate the molecular cascade leading to the hair follicle defects, our findings indicate that Bmp2, Bmp4 and Msx2 suppression occurs early in the process, while downregulation of other transcriptional regulators factors may be secondary events. Of note, the early entry in anagen, deficient hair differentiation and regeneration observed in K5-Myb mice resemble those observed upon Bmp inactivation (Botchkarev et al., 2001, Guha et al., 2004, Kulessa et al., 2000).

Epidermal hyperplasia and hyperkeratosis observed in K5-Myb mice resembles phenotypes that are often associated with early cutaneous tumor development, such as those induced by Ras mutations, a primary initiating event in skin carcinogenesis (Greenhalgh et al., 1993). Although skin tumors were not observed in K5-Myb mice during the current study, we cannot rule out that MYB activity may predispose to tumor development in the presence of some of the genetic alterations found in cutaneous malignancies, especially when considering that elevated levels of MYB expression and genomic rearrangements involving

the MYB gene have been observed in adnexal skin tumors (Evangelista and North, 2017, Pardal et al., 2017, Rajan et al., 2016, van der Horst et al., 2015).

MYB overexpression promoted proliferation in the epidermis, but not in hair follicles, while altered differentiation was found in both the epidermis and the hair follicles. These observations suggest that MYB may control differentiation processes in skin keratinocytes, and the epidermal proliferation and hair follicle stem cell depletion might be compensatory mechanisms to cope with the impaired differentiation.

The skin of K5-Myb mice was infiltrated with T cells (CD3+) and Tregs (FOXP3+), and exhibited gene expression programs that resemble those found in psoriasis, an inflammatory skin disorder. Moreover, additional phenotypes observed in K5-Myb mice, including hyperplasia, hyperkeratosis and a prominent cornified layer, were consistent with some of the main pathological features found in patients with psoriasis (Boehncke and Schon, 2015). Of note, the IL23 pathway was the most enriched pathway for genes upregulated in the skin of K5-Myb. This is remarkable because IL23 expression was found to be increased in psoriatic lesions, and genomic studies have implicated the IL23 signaling pathway in the development of psoriasis (Cargill et al., 2007, Lee et al., 2004, Nair et al., 2009, Nair et al., 2008). Interestingly, FOXP3 infiltration has been previously found to promote hair follicle regeneration by augmenting hair follicle stem cells proliferation and differentiation (Ali et al., 2017). As some of these mechanisms have been found altered in K5-Myb mice, further studies are warranted to determine whether the Treg infiltration contributes to the skin phenotypes promoted by MYB overexpression.

In summary, we generated a mouse model that revealed that deregulated MYB expression disrupts skin homeostasis, resulting in hair loss and phenotypic changes that resemble those found in psoriasis. Therefore, this mouse model may help to better understand the mechanisms underlying hair regeneration may also be used as a surrogate experimental model to test and refine new therapeutic strategies for psoriasis.

MATERIALS AND METHODS

Mouse models

The K5.CrePR1 and ROSA26-LSL-tTA (R26.ZtTA) mice have been previously described (Li et al., 2010, Zhou et al., 2002). The generation of TetO-Myb mice will be described elsewhere (manuscript in preparation). These mouse strains were bred to produce the experimental cohorts as indicated in Fig. S1 and Table S1. Littermates were used in all comparative studies. Mice were genotyped by PCR of genomic DNA purified from mouse tails. All animal studies were approved by The University of Texas MD Anderson Cancer Center and University of Arizona Institutional Animal Care and Use Committees.

Western Blot Analysis

Total protein was prepared by homogenizing skin samples in RIPA buffer (150 mM NaCl, 1% Triton X-100, 1% sodium deoxycholate, 0.1% SDS, and 50 mM Tris [pH 7.4]) with protease inhibitor cocktail (#78442, Thermo Scientific, Waltham, MA). Equal amounts of protein were separated in 10% SDS-PAGE gel, transferred to a polyvinylidene difluoride

membranes (Immobilon, Millipore, MA), blocked with 5% nonfat milk and incubated with primary antibodies (Table S5) overnight at 4°C. After three washes, membranes were incubated with secondary antibodies for 1h at room temperature (RT). The proteins were visualized using the Pierce™ ECL Western Blotting Substrate kit (Thermo Fisher, Waltham, MA).

Tissue processing and histology analyses

Mouse tissues were fixed in 10% neutral-buffered formalin at RT overnight, transferred to 75% ethanol and embedded in paraffin. Histologic sections (5μm) were stained with hematoxylin and eosin (H&E) or processed for immunohistochemistry (IHC), *in situ* hybridization (ISH) or immunofluorescence (IF). Myb iSH was carried out using the RNAScope system with specific probes (#510411, Advanced Cell Diagnostic, Newark, CA), per manufacturer's instructions, as previously described (Chen et al., 2015, Wang et al., 2012). IHC was performed using the Leica Bond RX automated stainer (Leica Biosystems Buffalo Grove, IL) in the Tissue Acquisition and Cellular/Molecular Analysis (TACMASR) (University of Arizona Cancer Center) using primary antibodies listed on Table S5. Staining for CD3 and FOXP3 was scored as the number of positive cells per mm^2, as previously described (Wang et al., 2017). IF was performed as described previously (Dai et al., 2013). Briefly, tissue sections were deparaffinized, rehydrated, and then microwaved in Tris-EDTA-Tween buffer (10 mM Tris Base, 1 mM EDTA, 0.05% Tween 20, pH 8.0) for 2 min for antigen retrieval. Sections were blocked in 10% BSA with 0.3% Triton-X 100 at RT for 30min, and then incubated with primary antibodies at 4°C overnight. Then AlexaFluor-488 or AlexaFluor-594 conjugated secondary antibodies (Thermo Fisher) were incubated at RT for 2h. Sections were sealed in mounting medium with 4′,6-diamidino-2-phenylindole (Vector Laboratories, Burlingame, CA). Microscopic images were captured on a Leica DMI microscope equipped with a Leica DCF450 camera (Leica Microsystems) or a Nikon Eclipse 80i (Melville, NY) microscope fitted with a Nikon DS-Qi1Mc camera and processed with Photoshop CS (Adobe, San Jose, CA).

RNA sequencing

RNA was purified from mouse skin using the RNeasy kit (#74104) from Qiagen (Valencia, CA), following manufacturer instructions. RNA sequencing was conducted at the Baylor College of Medicine Genomic and RNA Profiling Core. Quality checks were conducted using the NanoDrop ND-1000 spectrophotometer and Agilent Bioanalyzer 2100. The TruSeq Stranded Total RNA-Seq kit was used to create an Illumina library from 250ng of total RNA. The flowcell containing the clustered libraries were loaded on an Illumina HiSeq 2500 instrument along with the kitted SBS v3 sequencing reagents for a PE 100 bp run. After sequencing was complete, the CASAVA software converted the fluorescent dye values into sequence files.

Analysis of gene expression

Fastq files were uploaded in Galaxy (https://usegalaxy.org/) (Afgan et al., 2018) to conduct quality control with the FastQC tool, sequence alignment with HISAT2 and gene expression quantification with featureCounts. Differential gene expression was assessed using the DESeq package in Bioconductor (Anders and Huber, 2010). Differentially expressed genes

with adjusted p-value <0.01 and log2 fold >1.5 were used for downstream analysis with the ToppGene Suite (Chen et al., 2009) and GSEA analysis (Subramanian et al., 2005).

Real-Time quantitative reverse transcription-polymerase chain reaction

RevertAid First Strand cDNA Synthesis Kit (Thermo Fisher) was used to synthesize the first strand cDNA from the extracted RNA. The mRNA expression was evaluated using SYBRGreen PCR reagents (Thermo Fisher) following the manufacturer's instructions on a SingleOnePlus Applied Biosystems Thermocycler (Thermo Fisher) and specific primers for each gene (Table S6). The gene expression levels were normalized to Actin mRNA expression.

Supplementary Material

Refer to Web version on PubMed Central for supplementary material.

ACKNOWLEDGMENTS

This work was partially supported by the NIH grants R21DE023656 (CC), R01DE026735 (CC), R01AR061485 (JC), the Adenoid Cystic Carcinoma Research Foundation (CC), and the China Scholarship Council 201706010325 (ZS). Veterinary services and core facilities were supported by the NIH Cancer Center Support Grants P30CA016672 and P30CA023074. TACMASR facility was supported by the National Cancer Institute Cancer Center Support Grant P30CA023074.

REFERENCES

Adam RC, Yang H, Ge Y, Lien WH, Wang P, Zhao Y, et al. Temporal Layering of Signaling Effectors Drives Chromatin Remodeling during Hair Follicle Stem Cell Lineage Progression. Cell Stem Cell 2018;22(3):398–413.e7. [PubMed: 29337183]

Afgan E, Baker D, Batut B, van den Beek M, Bouvier D, Cech M, et al. The Galaxy platform for accessible, reproducible and collaborative biomedical analyses: 2018 update. Nucleic Acids Res 2018;46(W1):W537–w44. [PubMed: 29790989]

Ali N, Zirak B, Rodriguez RS, Pauli ML, Truong HA, Lai K, et al. Regulatory T Cells in Skin Facilitate Epithelial Stem Cell Differentiation. Cell 2017;169(6):1119–29.e11. [PubMed: 28552347]

Alsaad KO, Obaidat NA, Ghazarian D. Skin adnexal neoplasms--part 1: an approach to tumours of the pilosebaceous unit. J Clin Pathol 2007;60(2):129–44. [PubMed: 16882696]

Anders S, Huber W. Differential expression analysis for sequence count data. Genome Biol 2010;11(10):R106. [PubMed: 20979621]

Blanpain C, Fuchs E. Epidermal homeostasis: a balancing act of stem cells in the skin. Nature reviews Molecular cell biology 2009;10(3):207–17. [PubMed: 19209183]

Boehncke WH, Schon MP. Psoriasis. Lancet 2015;386(9997):983–94. [PubMed: 26025581]

Botchkarev VA, Botchkareva NV, Nakamura M, Huber O, Funa K, Lauster R, et al. Noggin is required for induction of the hair follicle growth phase in postnatal skin. Faseb j 2001;15(12):2205–14. [PubMed: 11641247]

Cargill M, Schrodi SJ, Chang M, Garcia VE, Brandon R, Callis KP, et al. A large-scale genetic association study confirms IL12B and leads to the identification of IL23R as psoriasis-risk genes. American journal of human genetics 2007;80(2):273–90. [PubMed: 17236132]

Chen J, Bardes EE, Aronow BJ, Jegga AG. ToppGene Suite for gene list enrichment analysis and candidate gene prioritization. Nucleic Acids Res 2009;37(Web Server issue):W305–11. [PubMed: 19465376]

Chen J, Laclef C, Moncayo A, Snedecor ER, Yang N, Li L, et al. The ciliopathy gene Rpgrip1l is essential for hair follicle development. J Invest Dermatol 2015;135(3):701–9. [PubMed: 25398052]

Cheng JB, Sedgewick AJ, Finnegan AI, Harirchian P, Lee J, Kwon S, et al. Transcriptional Programming of Normal and Inflamed Human Epidermis at Single-Cell Resolution. Cell reports 2018;25(4):871–83. [PubMed: 30355494]

Dai D, Li L, Huebner A, Zeng H, Guevara E, Claypool DJ, et al. Planar cell polarity effector gene Intu regulates cell fate-specific differentiation of keratinocytes through the primary cilia. Cell death and differentiation 2013;20(1):130–8. [PubMed: 22935613]

Eckhart L, Lippens S, Tschachler E, Declercq W. Cell death by cornification. Biochimica et biophysica acta 2013;1833(12):3471–80. [PubMed: 23792051]

Ess KC, Witte DP, Bascomb CP, Aronow BJ. Diverse developing mouse lineages exhibit high-level c-Myb expression in immature cells and loss of expression upon differentiation. Oncogene 1999;18(4): 1103–11. [PubMed: 10023687]

Evangelista MT, North JP. MYB, CD117 and SOX-10 expression in cutaneous adnexal tumors. Journal of cutaneous pathology 2017;44(5):444–50. [PubMed: 28098399]

Godwin AR, Capecchi MR. Hoxc13 mutant mice lack external hair. Genes Dev 1998; 12(1):11–20. [PubMed: 9420327]

Greenhalgh DA, Rothnagel JA, Quintanilla MI, Orengo CC, Gagne TA, Bundman DS, et al. Induction of epidermal hyperplasia, hyperkeratosis, and papillomas in transgenic mice by a targeted v-Ha-ras oncogene. Mol Carcinog 1993;7(2):99–110. [PubMed: 7681293]

Guha U, Mecklenburg L, Cowin P, Kan L, O'Guin WM, D'Vizio D, et al. Bone morphogenetic protein signaling regulates postnatal hair follicle differentiation and cycling. Am J Pathol 2004;165(3):729–40. [PubMed: 15331398]

Horsley V, Aliprantis AO, Polak L, Glimcher LH, Fuchs E. NFATc1 balances quiescence and proliferation of skin stem cells. Cell 2008;132(2):299–310. [PubMed: 18243104]

Jiang TX, Liu YH, Widelitz RB, Kundu RK, Maxson RE, Chuong CM. Epidermal dysplasia and abnormal hair follicles in transgenic mice overexpressing homeobox gene MSX-2. J Invest Dermatol 1999;113(2):230–7. [PubMed: 10469309]

Joost S, Zeisel A, Jacob T, Sun X, La Manno G, Lonnerberg P, et al. Single-Cell Transcriptomics Reveals that Differentiation and Spatial Signatures Shape Epidermal and Hair Follicle Heterogeneity. Cell systems 2016;3(3):221–37.e9. [PubMed: 27641957]

Kobielak K, Stokes N, de la Cruz J, Polak L, Fuchs E. Loss of a quiescent niche but not follicle stem cells in the absence of bone morphogenetic protein signaling. Proc Natl Acad Sci U S A 2007;104(24):10063–8. [PubMed: 17553962]

Kulessa H, Turk G, Hogan BL. Inhibition of Bmp signaling affects growth and differentiation in the anagen hair follicle. Embo j 2000;19(24):6664–74. [PubMed: 11118201]

Lee E, Trepicchio WL, Oestreicher JL, Pittman D, Wang F, Chamian F, et al. Increased expression of interleukin 23 p19 and p40 in lesional skin of patients with psoriasis vulgaris. J Exp Med 2004;199(1):125–30. [PubMed: 14707118]

Li L, Tasic B, Micheva KD, Ivanov VM, Spletter ML, Smith SJ, et al. Visualizing the distribution of synapses from individual neurons in the mouse brain. PLoS One 2010;5(7):e11503. [PubMed: 20634890]

Lim X, Nusse R. Wnt signaling in skin development, homeostasis, and disease. Cold Spring Harbor perspectives in biology 2013;5(2).

Liu Y, Lyle S, Yang Z, Cotsarelis G. Keratin 15 promoter targets putative epithelial stem cells in the hair follicle bulge. J Invest Dermatol 2003;121(5):963–8. [PubMed: 14708593]

Liu Y, Snedecor ER, Zhang X, Xu Y, Huang L, Jones EC, et al. Correction of Hair Shaft Defects through Allele-Specific Silencing of Mutant Krt75. J Invest Dermatol 2016;136(1):45–51. [PubMed: 26763422]

Lopez-Pajares V, Yan K, Zarnegar BJ, Jameson KL, Khavari PA. Genetic pathways in disorders of epidermal differentiation. Trends Genet 2013;29(1):31–40. [PubMed: 23141808]

Millar SE. Molecular mechanisms regulating hair follicle development. J Invest Dermatol 2002;118(2):216–25. [PubMed: 11841536]

Mills KJ, Robinson MK, Sherrill JD, Schnell DJ, Xu J. Analysis of gene expression profiles of multiple skin diseases identifies a conserved signature of disrupted homeostasis. Experimental dermatology 2018;27(9):1000–8. [PubMed: 29806976]

Nair RP, Duffin KC, Helms C, Ding J, Stuart PE, Goldgar D, et al. Genome-wide scan reveals association of psoriasis with IL-23 and NF-kappaB pathways. Nat Genet 2009;41(2):199–204. [PubMed: 19169254]

Nair RP, Ruether A, Stuart PE, Jenisch S, Tejasvi T, Hiremagalore R, et al. Polymorphisms of the IL12B and IL23R genes are associated with psoriasis. J Invest Dermatol 2008;128(7):1653–61. [PubMed: 18219280]

Pardal J, Sundram U, Selim MA, Hoang MP. GATA3 and MYB Expression in Cutaneous Adnexal Neoplasms. The American Journal of dermatopathology 2017;39(4):279–86. [PubMed: 28323779]

Rajan N, Andersson MK, Sinclair N, Fehr A, Hodgson K, Lord CJ, et al. Overexpression of MYB drives proliferation of CYLD-defective cylindroma cells. J Pathol 2016;239(2):197–205. [PubMed: 26969893]

Rendl M, Polak L, Fuchs E. BMP signaling in dermal papilla cells is required for their hair follicle-inductive properties. Genes Dev 2008;22(4):543–57. [PubMed: 18281466]

Rhee H, Polak L, Fuchs E. Lhx2 maintains stem cell character in hair follicles. Science 2006;312(5782): 1946–9. [PubMed: 16809539]

Subramanian A, Tamayo P, Mootha VK, Mukherjee S, Ebert BL, Gillette MA, et al. Gene set enrichment analysis: a knowledge-based approach for interpreting genome-wide expression profiles. Proc Natl Acad Sci U S A 2005; 102(43):15545–50. [PubMed: 16199517]

Tkatchenko AV, Visconti RP, Shang L, Papenbrock T, Pruett ND, Ito T, et al. Overexpression of Hoxc13 in differentiating keratinocytes results in downregulation of a novel hair keratin gene cluster and alopecia. Development 2001; 128(9): 1547–58. [PubMed: 11290294]

Trempus CS, Morris RJ, Bortner CD, Cotsarelis G, Faircloth RS, Reece JM, et al. Enrichment for living murine keratinocytes from the hair follicle bulge with the cell surface marker CD34. J Invest Dermatol 2003;120(4):501–11. [PubMed: 12648211]

Tumbar T, Guasch G, Greco V, Blanpain C, Lowry WE, Rendl M, et al. Defining the epithelial stem cell niche in skin. Science 2004;303(5656):359–63. [PubMed: 14671312]

van der Horst MP, Marusic Z, Hornick JL, Luzar B, Brenn T. Morphologically low-grade spiradenocarcinoma: a clinicopathologic study of 19 cases with emphasis on outcome and MYB expression. Modern pathology : an official journal of the United States and Canadian Academy of Pathology, Inc 2015;28(7):944–53.

Vesela B, Svandova E, Smarda J, Matalova E. Mybs in mouse hair follicle development. Tissue & cell 2014;46(5):352–5. [PubMed: 25064514]

Wang F, Flanagan J, Su N, Wang LC, Bui S, Nielson A, et al. RNAscope: a novel in situ RNA analysis platform for formalin-fixed, paraffin-embedded tissues. The Journal of molecular diagnostics : JMD 2012;14(1):22–9. [PubMed: 22166544]

Wang J, Xie T, Wang B, William WN Jr., Heymach JV, El-Naggar AK, et al. PD-1 Blockade Prevents the Development and Progression of Carcinogen-Induced Oral Premalignant Lesions. Cancer prevention research (Philadelphia, Pa) 2017;10(12):684–93.

Yang H, Adam RC, Ge Y, Hua ZL, Fuchs E. Epithelial-Mesenchymal Micro-niches Govern Stem Cell Lineage Choices. Cell 2017;169(3):483–96.e13. [PubMed: 28413068]

Zhang J, He XC, Tong WG, Johnson T, Wiedemann LM, Mishina Y, et al. Bone morphogenetic protein signaling inhibits hair follicle anagen induction by restricting epithelial stem/progenitor cell activation and expansion. Stem Cells 2006;24(12):2826–39. [PubMed: 16960130]

Zhou Z, Wang D, Wang XJ, Roop DR. In utero activation of K5.CrePR1 induces gene deletion. Genesis 2002;32(2):191–2. [PubMed: 11857819]

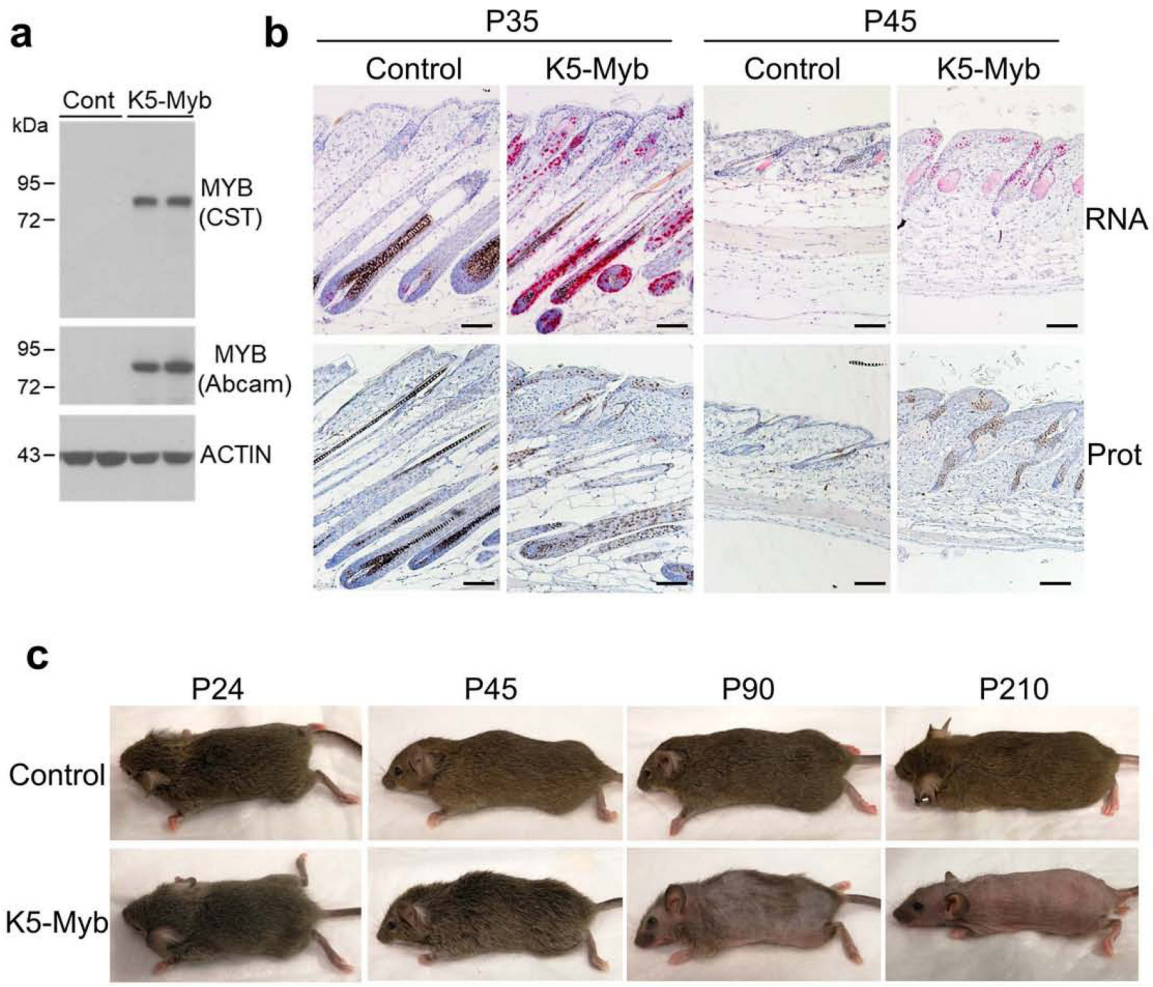

Figure 1.

Overexpression of MYB in the skin induces hair loss. (a) Western blot for MYB on skin samples from control and K5-Myb mice at P55, using two different antibodies CST (# 12319S) and Abcam (# ab45150). (b) *Myb* mRNA expression detected by in situ hybridization (top panels) and immunohistochemistry for MYB protein (Prot, bottom panels) in the skin of control and K5-Myb mice. Scale bar= 100μm. (c) Gross appearance of control and K5-Myb mice at the indicated time points. Images are representative of at least 3 mice per group and time point.

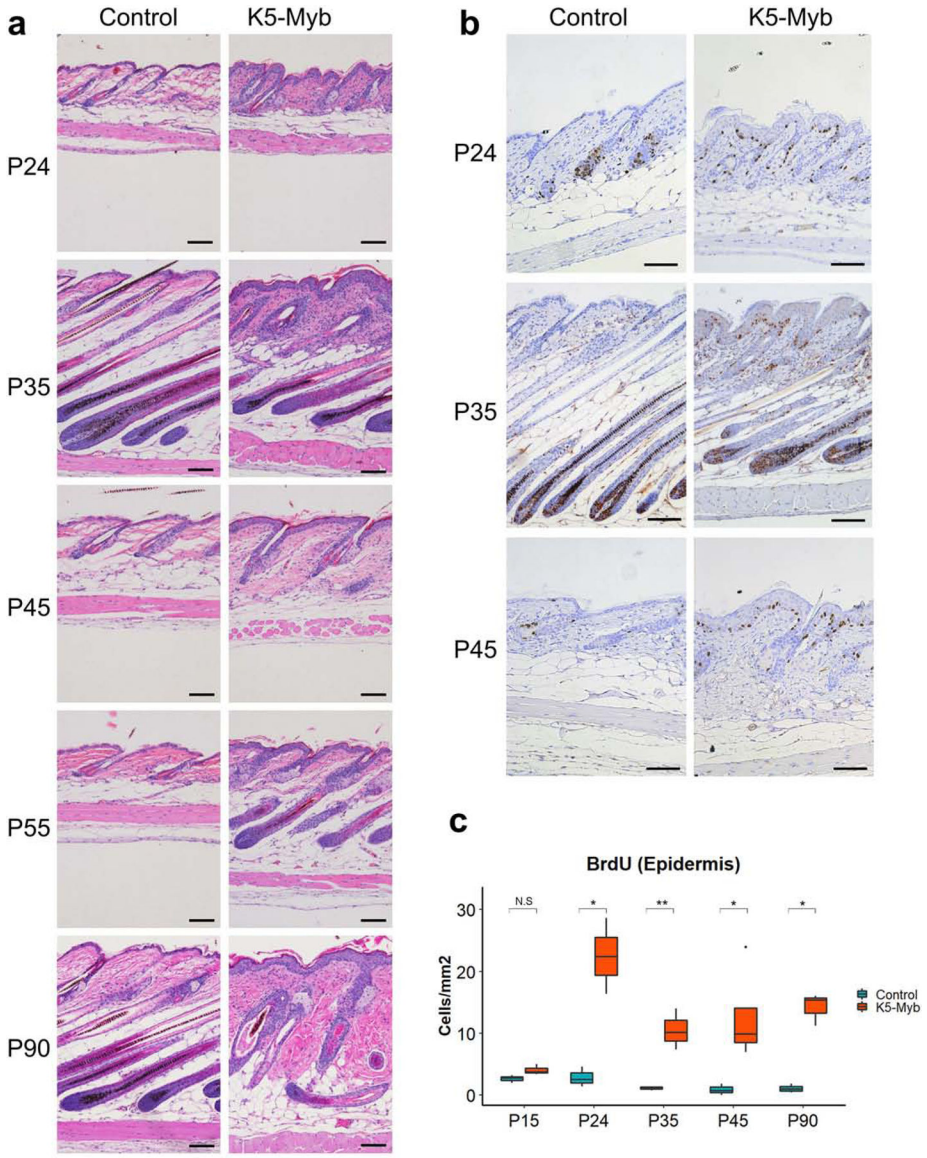

Figure 2.

MYB overexpression induces hyperplasia and hyperkeratosis in the epidermis. (a) H&E staining of the skin of control and K5-Myb mice at the indicated time points. Scale bar= 100μm. (b) Immunohistochemistry analysis for BrdU. Scale bar=100μm. (c) Quantification of the BrdU staining for each time point in the epidermis (n=3). *p<0.05, **p<0.005, N.S (not significant)

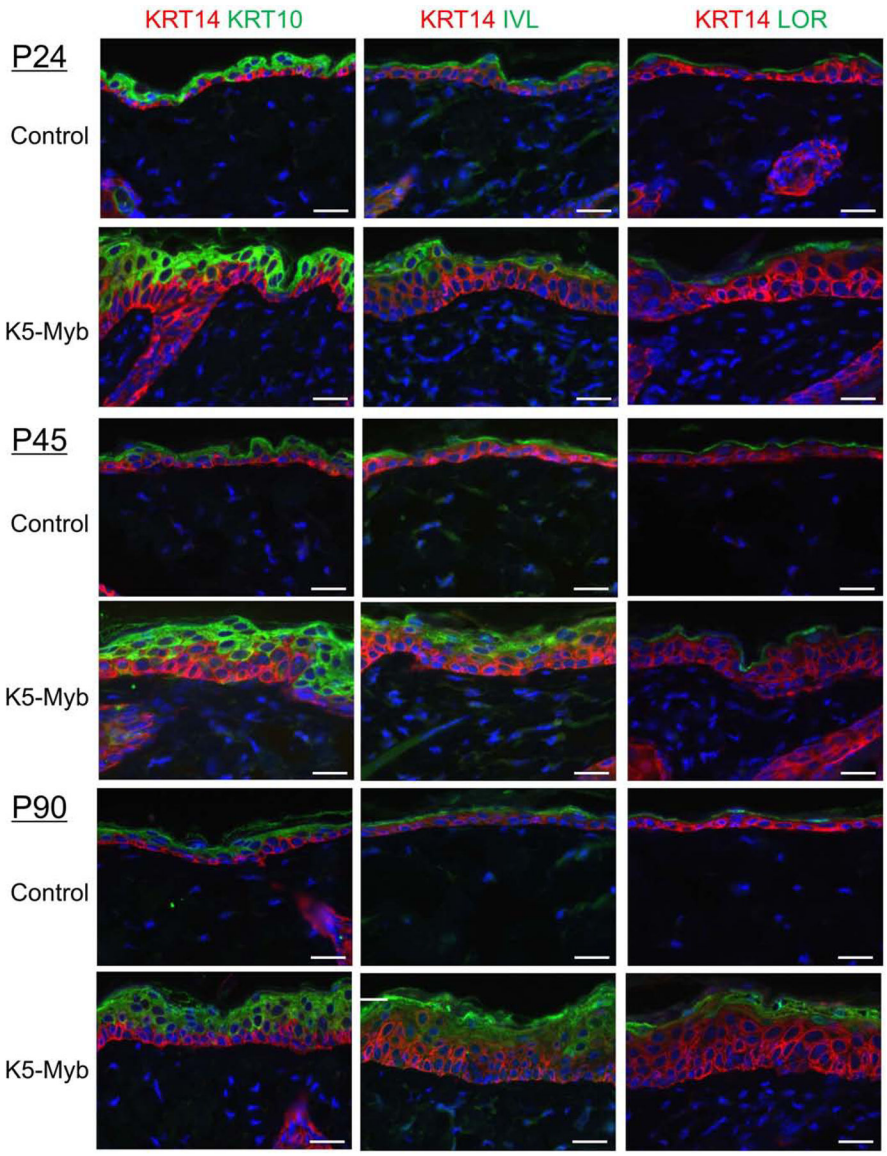

Figure 3.

Aberrant expression of epidermal differentiation markers in K5-Myb skin. Double immunofluorescence for the basal layer maker KRT14, and KRT10, INV or LOR in control and K5-Myb mice, at P24, P45 and P90, as indicated. Images are representative of 3 mice per group and time point. Scale bar= 20μm.

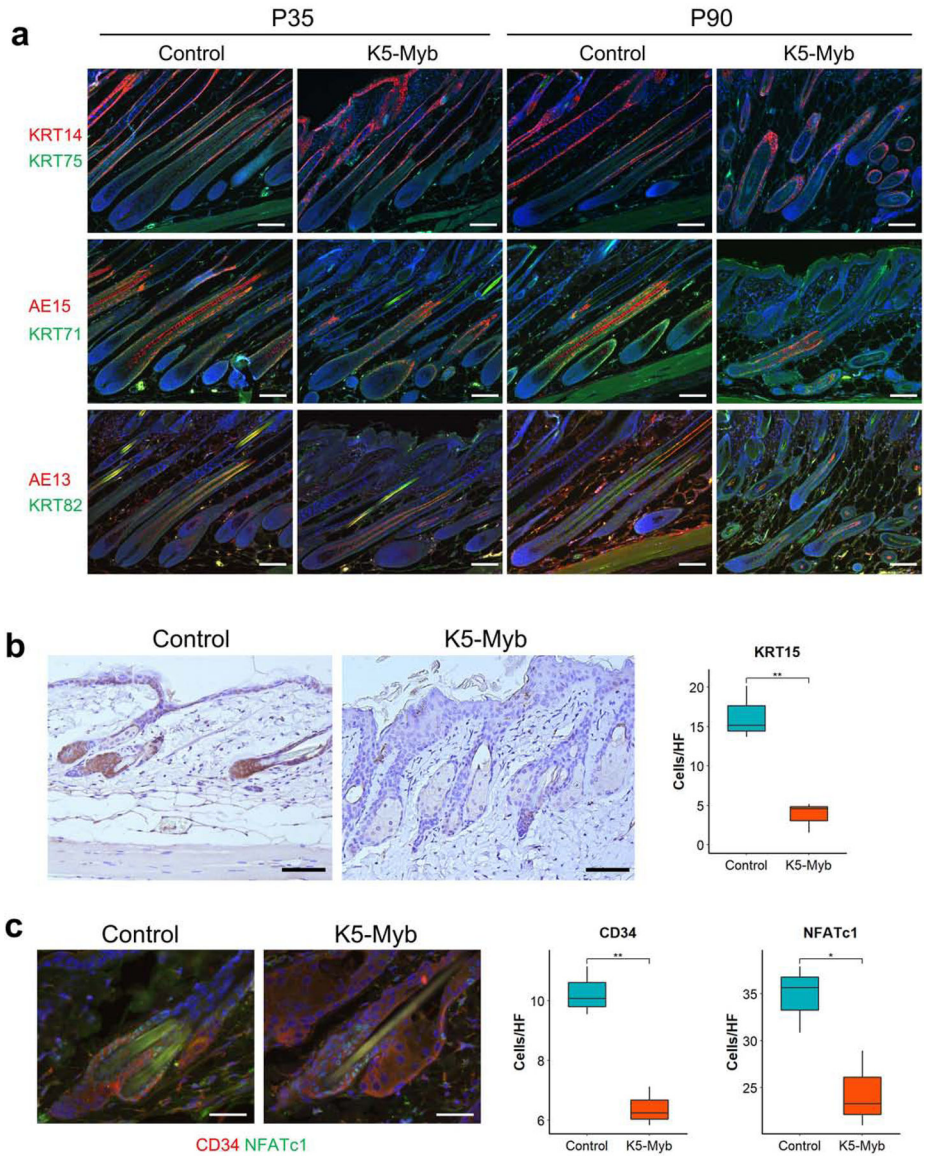

Figure 4.

Altered hair follicle differentiation and stem cell depletion in K5-Myb skin. (a) Double immunofluorescence for the indicated hair follicles markers, in hair follicles from control and K5-Myb mice, at P35 and P90, as indicated. Scale bar= 50μm. (b) Immunohistochemistry for KRT15 and quantification of the number of KRT15 positive cells per hair follicle (HF) at P45 (n=3). Scale bar= 100μm. (c) Double immunofluorescence for NFATc1 and CD34 in hair follicles of control and K5-Myb mice at P45, and quantification of the number of positive cells for each marker (n=3) *p<0.05, **p<0.005. Scale bar= 20μm.

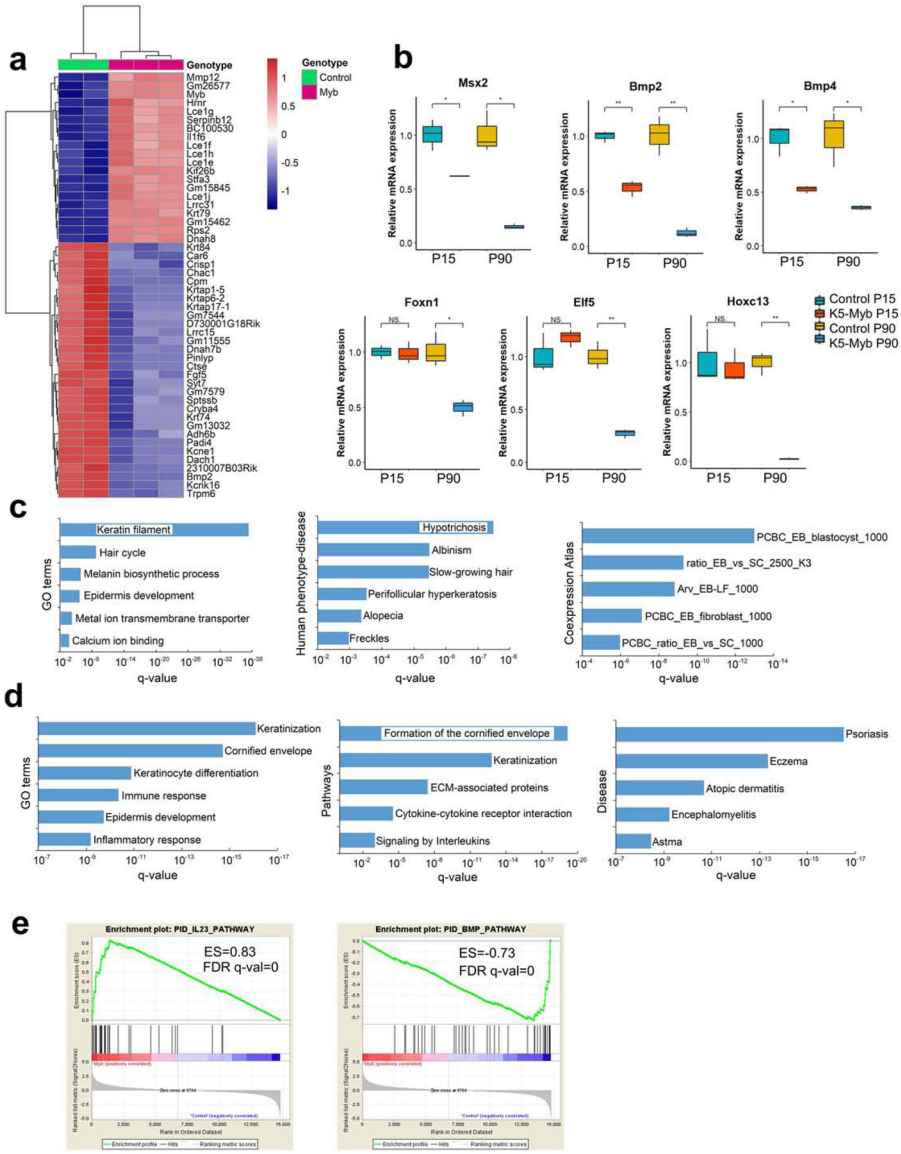

Figure 5.

Gene expression profiles induced by MYB overexpression in the skin. (a) Heatmap of the 100 most differentially expressed genes between the skin of control and K5-Myb mice. (b) Quantitative RT-PCR for the indicated genes in the skin of control and K5-Myb mice at P15 and P90 (n=3). (c) Enrichment for functional terms in genes downregulated in the skin of K5-Myb mice compared to controls. (c) Enrichment for functional terms in genes upregulated in the skin of K5-Myb mice compared to controls. (d) GSEA analysis showing the top pathways enriched in genes upregulated (left panel) or downregulated (right panel) in the skin of K5-Myb mice. *p<0.05, **p<0.005, N.S (not significant).

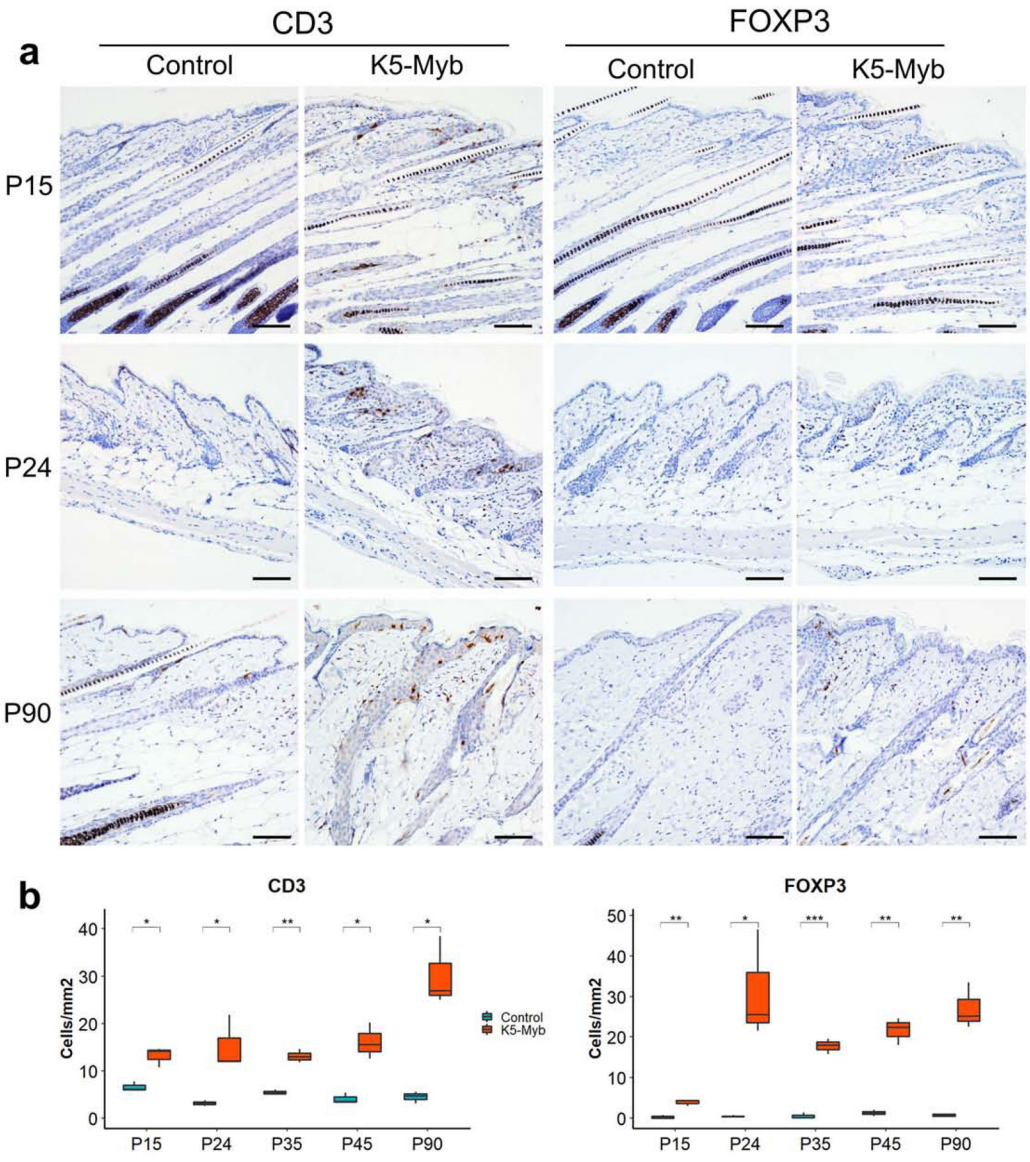

Figure 6.

MYB promotes T-cell infiltration in the skin. (a) Immunohistochemistry for CD3 and FOXP3 in control and K5-Myb mice. Scale bar= 100μm. (b) Quantification for each marker is shown on the graphs on the right panels (n=3). *p<0.05, **p<0.005, ***p<0.0005.